IET Radar, Sonar & Navigation

Research Article

On the design of staggered moving target indicator filters

ISSN 1751-8784
Received on 28th October 2014
Revised on 27th May 2015
Accepted on 27th June 2015
doi: 10.1049/iet-rsn.2015.0175
www.ietdl.org

Mehmet Ispir[1] ✉, *Cagatay Candan*[2]

[1]*ILTAREN, TUBITAK BILGEM, Ankara, Turkey*
[2]*Department of Electrical and Electronics Engineering, Middle East Technical University (METU), Ankara, Turkey*
✉ *E-mail: mehmet.ispir@tubitak.gov.tr*

Abstract: The problem of moving target indicator (MTI) filter design for radar systems with non-uniform (staggered) pulse repetition intervals is examined. The goal is to realise and then utilise a trade-off in the design of MTI filter between the conflicting requirements of high suppression of undesired signal (clutter echo) and minimal suppression of desired signal (target echo). To that aim, three design methodologies, namely, least squares, convex optimisation and min–max error, are studied. The numerical results indicate that the presented designs yield high-performance MTI filters which are easily applicable to a variety of operational scenarios. A ready-to-use source code for the design of suggested filters is also provided.

1 Introduction

Moving target indication (MTI) filters are designed to improve the detection probability of moving targets by suppressing the stationary clutter return. The simplest and most well-known MTI filter is the single line canceller which subtracts the received signal due to two consecutive pulses in order to cancel the clutter. The simplicity of MTI filtering and its satisfactory performance in several applications makes this operation a frequent choice in many systems. An important disadvantage associated with MTI filtering is the blind speed problem that results from the usage of constant pulse repetition interval (PRI). Moving targets with the Doppler frequencies matching the null frequency, which is an integer multiple of 1/PRI hertz, are also cancelled along with the clutter return. The range rates corresponding to these specific frequencies are called *blind speeds* [1]. A remedy to the blind speed problem is the usage of staggered PRIs [2]. With this solution, the first blind speed of the system is increased and a wider Doppler frequency range is covered. This paper presents three different approaches for MTI filter design for the systems with non-uniform PRI.

A typical frequency response curve for uniform and staggered MTI operations is given in Fig. 1. Fig. 1 shows that the response of the staggered system has undesired fluctuations in the passband. These fluctuations can be of several decibels and may result in a significant decrease of detection probability at some specific Doppler frequencies. To improve the detection probability, the fluctuations in the passband should be minimised, and at the same time the clutter suppression performance around the DC frequency should be sufficiently large.

The majority of MTI filter designs in the literature are developed for the uniform PRI operation [3–5]. The non-uniform case seems to attract less attention due to its dependency on the application scenario, that is, the utilised set of PRI values [6, 7]. One of the first methods for non-uniform operation is developed by Prinsen [3]. Prinsen suggests to adjust the filter weights to provide maximally flat stopband characteristics at DC frequency. The approach of Prinsen relies on the Taylor series expansion of the frequency response at the zero frequency and can be considered as the dual of single line canceller systems, that is, $H(z) = 1 - z^{-1}$, for non-uniform PRI systems. In a later work, Prinsen suggests the optimisation of the stagger periods with the filter weights [4]. In [8], Hsiao has suggested the optimisation of the filter weights with the objective of the flat passband along with the constraint of maximum stopband attenuation (SA). Jacomini uses the same constraints of Hsiao, but suggests a change in the cost function to assist the computation of the filter as described in [9]. Neither the work of Hsiao nor the work Jacomini does establish a trade-off between the desired responses in passband and stopband.

In this paper, we apply three widely adopted finite impulse response (FIR) filter design techniques in the signal processing literature, namely, the least squares (LSs), convex optimisation and min–max (MM) filter design; to the design of non-uniform MTI filters. Our goal is to obtain maximum amount of clutter suppression concurrently with the least amount desired signal suppression (flat passband). To assist readers, ready-to-use MATLAB codes for all three design methodologies are provided in [10]. The provided codes can be used to generate filters for different operational settings such as PRI values, stopband passband specifications etc.

This paper is organised as follows: we first present a brief information on the staggered MTI operation; then a formulation for the frequency response calculation for the non-uniformly sampled signals is given. The filter design methodologies are described next and some numerical comparisons with the optimal designs known in the literature are given. The final section presents a summary of the work and also the conclusions.

2 Preliminaries

MTI filters for non-uniform PRI (staggered PRI) operation are designed to extend the first blind speed associated with the target echo. Doppler frequency corresponding to the first blind speed can be written as $f_b = \text{l.c.m.}(\text{PRF}_1, \text{PRF}_2, \ldots, \text{PRF}_L)$ [11]. Here PRF = 1/PRI denotes the pulse repetition frequency and l.c.m. denotes the lowest common multiple of the arguments. For the uniform PRI case, $\text{PRF}_1 = \text{PRF}_2 = \ldots = \text{PRF}_L = \text{PRF}$, the first blind speed coincides with the utilised PRF whose value can be low in comparison to some target speeds of interest. For example, weather radars typically utilise low PRF values to avoid target/clutter folding. For such systems, the low PRF values may reduce the first blind speed to an unacceptable value unless staggering option is utilised. A weather radar system utilising staggered PRFs of 3 and 4 kHz can cover Doppler frequencies up to 12 kHz and this range can be sufficient to cover many meteorological target

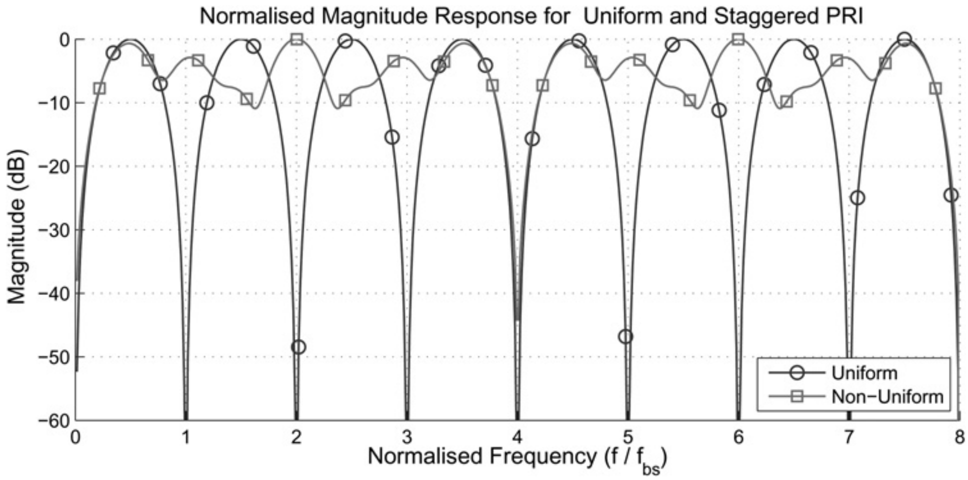

Fig. 1 *Comparison of frequency responses for uniform and non-uniform MTI filters* (f_{bs} *is the first blind speed of uniform MTI filter)*

speeds of interest. In this paper, our focus is not on the selection of PRF values; however, on the design of a 'suitable' MTI filters for a given set of PRF values.

We would like to briefly discuss the 'suitability' of an MTI filter to an application. An MTI filter can be considered to be suitable if the clutter strength (typically expressed in clutter-to-noise ratio) and clutter spectral width matches the stopband specifications of the filter. In practice, the radar operator/system selects a suitable MTI filter among the set of pre-designed filters according to the needs of operational scenario. As an example, if the clutter signal is weak (in comparison with the noise variance), there may be no need for the application of an MTI filter and the Doppler processing can be implemented without MTI filtering. On the other hand, in the presence of strong clutter, a suitable MTI filter can significantly improve the target detection performance.

In the present paper, we present a set of methodologies for the design of MTI filters. The effectiveness of the designs is studied from two different viewpoints. The first viewpoint treats the problem as a filter design problem and examines several criterion on the frequency response of the filter such as SA, passband ripple etc. The second viewpoint treats the problem as a radar signal processing problem and examines the MTI improvement factor (IF) which is the change in signal-to-clutter ratio (SCR) before and after filtering, that is, $\mathrm{IF} = (\mathrm{SCR})_{\mathrm{output}}/(\mathrm{SCR})_{\mathrm{input}}$.

We consider the signal model $\boldsymbol{r} = \boldsymbol{s}(\omega) + \boldsymbol{c} + \boldsymbol{n}$ where $\boldsymbol{r}$ is an $N \times 1$ column vector containing the slow-time samples of the return echo corresponding to a specific range-cell. Here N is the number of transmitted pulses which can be staggered or not. The vector $\boldsymbol{s}(\omega)$ denotes the desired signal which is the return due to target having the Doppler frequency ω. The vector $\boldsymbol{c}$ denotes the return due to clutter and the vector $\boldsymbol{n}$ denotes the white noise.

The goal of MTI processing is to linearly combine N samples of the vector $\boldsymbol{r}$ to reduce the contribution of the clutter at the output. The $N \times 1$ vector $\boldsymbol{w}$ can be considered as a set of linear combination coefficients to this aim. With these definitions MTI output can be written as $(\mathrm{MTI}_{\mathrm{output}}) = \boldsymbol{w}^{\mathrm{H}}\boldsymbol{r} = \boldsymbol{w}^{\mathrm{H}}\boldsymbol{s}(\omega) + \boldsymbol{w}^{\mathrm{H}}\boldsymbol{c} + \boldsymbol{w}^{\mathrm{H}}\boldsymbol{n}$ and the input and output SCR values can be expressed as follows:

$$(\mathrm{SCR})_{\mathrm{input}} = \frac{E\{\boldsymbol{s}(\omega)^{\mathrm{H}}\boldsymbol{s}(\omega)\}}{E\{\boldsymbol{c}^{\mathrm{H}}\boldsymbol{c}\}} = \frac{\sigma_{\mathrm{s}}^2}{\sigma_{\mathrm{c}}^2}, \qquad (1)$$

$$(\mathrm{SCR})_{\mathrm{output}} = \frac{E\{|\boldsymbol{w}^{\mathrm{H}}\boldsymbol{s}(\omega)|^2)\}}{E\left\{|\boldsymbol{w}^{\mathrm{H}}\boldsymbol{c})|^2\right\}} = \frac{\boldsymbol{w}^{\mathrm{H}}\boldsymbol{R}_{\mathrm{s}}\boldsymbol{w}}{\boldsymbol{w}^{\mathrm{H}}\boldsymbol{R}_{\mathrm{c}}\boldsymbol{w}}. \qquad (2)$$

Here, the target signal $\boldsymbol{s}(\omega)$ and clutter signal $\boldsymbol{c}$ are assumed to have an auto-correlation matrixes $\boldsymbol{R}_{\mathrm{s}}$ and $\boldsymbol{R}_{\mathrm{c}}$, respectively. Similarly, the variables σ_{s}^2 and σ_{c}^2 are the variances of target and clutter. The MTI IF for the target with the Doppler frequency ω can then be written as

$$\mathrm{IF}(\omega) = \frac{(\mathrm{SCR})_{\mathrm{output}}}{(\mathrm{SCR})_{\mathrm{input}}} = \frac{\boldsymbol{w}^{\mathrm{H}}(1/\sigma_s^2)\boldsymbol{R}_{\mathrm{s}}\boldsymbol{w}}{\boldsymbol{w}^{\mathrm{H}}(1/\sigma_{\mathrm{c}}^2)\boldsymbol{R}_{\mathrm{c}}\boldsymbol{w}} = \frac{\boldsymbol{w}^{\mathrm{H}}\boldsymbol{R}_{\mathrm{s}n}\boldsymbol{w}}{\boldsymbol{w}^{\mathrm{H}}\boldsymbol{R}_{\mathrm{c}n}\boldsymbol{w}}. \qquad (3)$$

In (3), the matrices $\boldsymbol{R}_{\mathrm{s}n} = (1/\sigma_{\mathrm{s}}^2)\boldsymbol{R}_{\mathrm{s}}$ and $\boldsymbol{R}_{\mathrm{c}n} = (1/\sigma_{\mathrm{c}}^2)\boldsymbol{R}_{\mathrm{c}}$, with unit valued diagonals, correspond to the normalised version of signal and clutter auto-correlation matrices. A legitimate goal in the MTI filter design is the maximisation of $\mathrm{IF}(\omega)$.

In the present discussion, the target is assumed to be Swerling-0 or Swerling-1 type; stated differently, it is assumed that there is no target fluctuation during the coherent processing interval. Hence, the slow-time samples due to the target echo can be written as $\boldsymbol{s}(\omega) = \gamma_{\mathrm{s}}\boldsymbol{u}(\omega)$. Here, γ_{s} is a non-random quantity for Swerling-0 model and Rayleigh distributed for Swerling-1 model. The real valued γ_{s} parameter denotes the amplitude of the slow-time samples. The vector $\boldsymbol{u}$, appearing in the relation $\boldsymbol{s}(\omega) = \gamma_{\mathrm{s}}\boldsymbol{u}(\omega)$, is formed by the phase of the slow-time samples. With this model, the normalised auto-correlation matrix for the desired signal is a rank 1 matrix which can be expressed as $\boldsymbol{R}_{\mathrm{s}n} = \boldsymbol{u}(\omega)\boldsymbol{u}(\omega)^{\mathrm{H}}$.

The clutter signal is assumed to have a Gaussian distributed power spectral density

$$P_{\mathrm{c}}(f) = \frac{\sigma_{\mathrm{c}}^2}{\sqrt{2\pi\sigma_g^2}} \exp\left(-\frac{f^2}{2\sigma_g^2}\right). \qquad (4)$$

The parameter σ_g appearing in this definition is the parameter of the density associated with the clutter Doppler spread. This parameter can be interpreted as the standard deviation of the clutter Doppler spread. The Gaussian distributed power spectral density model is particularly suitable for the radar systems with rotary antennas, such as weather radar systems, where the modulation of the clutter signal is mainly due to the antenna scanning.

3 Non-uniform MTI filter design

The filtering structure for the FIR staggered MTI operation is shown in Fig. 2. Here, the output signal $y(t)$ is formed by a linear combination of the non-uniformly sampled input signal.

The frequency response of this system can be expressed as

$$H(f) = \sum_{n=0}^{N} \alpha_n \mathrm{e}^{-\mathrm{j}2\pi f\, t_n} \qquad (5)$$

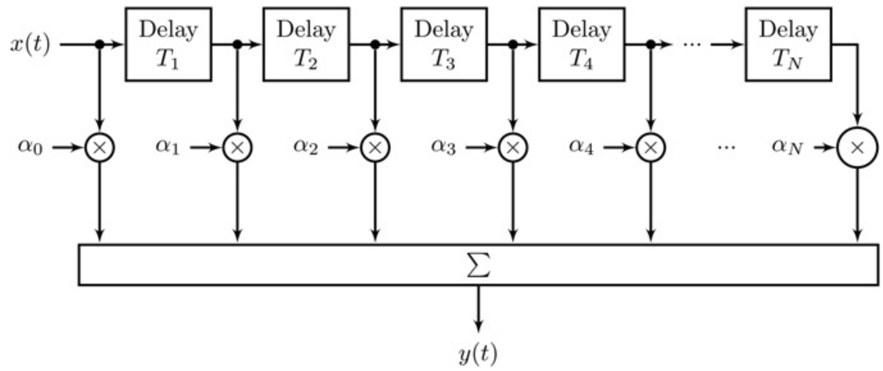

Fig. 2 *Filtering structure for non-uniform MTI processor*

where the definition for t_n is

$$t_n = \begin{cases} \sum_{i=0}^{n-1} T_i, & n \geq 1 \\ 0, & n = 0 \end{cases} \tag{6}$$

Here f denotes the frequency in hertz, α_n is the nth filter coefficient and t_n is the nth sampling time instant whose value is given in (6). It should be noted that T_i's correspond to the interpulse periods for the radar signal processing application.

The ideal frequency response for a staggered MTI system is illustrated in Fig. 3. The high-pass part of the spectrum shown in Fig. 3 is divided into three frequency regions. *Clutter region* starts from DC and goes up to the cut-off frequency and forms the stopband. The *transition region* is the second region and identifies the steepness of the MTI filter. The third region is the *velocity region* indicating the Doppler frequency of the interested targets and it is the passband of the MTI filter.

The goal in MTI filter design is to minimise the passband ripple (to provide small signal-to-noise ratio loss for the targets in the velocity region) and to provide sufficiently high clutter attenuation (to minimise the effect of clutter signal at the output). We note that both objectives cannot be improved simultaneously and a practical solution has to operate at a trade-off between these objectives. The trade-off between these objectives depends on the optimisation of two sets of parameters: the interpulse time durations (T_i) and filter coefficients (α_i). To evaluate and compare different trade-off points objectively, some quantitative performance criterions are needed. The following presents the performance criterion utilised in this paper [12].

SA at f_c: SA is the value of filter magnitude response at the cut-off frequency f_c. Since the frequency values smaller than f_c ($0 \leq f \leq f_c$) are typically attenuated more than the value at the cut-off frequency, this value can be considered to represent the worst-case clutter attenuation in the stopband. This criterion can be expressed as $\mathrm{SA} = |H(f_c)|^2$.

Maximum deviation (MD): This criterion indicates the MD from the ideal flat response in the velocity region. The MD value is commonly seen around the transition region and referred as *the depth of the first null*. This criterion can be expressed as $\mathrm{MD} = \max\, |H_d(f) - H(f)|^2$.

Mean passband error (MPE): This criterion is given to measure the flatness of the filter response in the velocity region. It is based on the difference between ideal and designed filter responses in the passband and given by $\mathrm{MPE} = \int_{f_t}^{f_p} |H_d(f) - H(f)|^2\, df$, where $H_d(f)$ and $H(f)$ are the frequency responses of the ideal and designed filters, respectively. The limits of the integral are the lowest and highest frequencies in the velocity region as shown in Fig. 3.

Fig. 4 illustrates the criterion used in this paper. As a cautionary remark, we note that the maximum frequency value for the desired passband (f_p in Fig. 4) must be smaller than $f_{max} - f_c$ for a proper optimisation. This consideration is due to the periodicity of clutter spectrum. Here, f_{max} denotes the blind speed of the staggered MTI system, as discussed in Section 2.

To provide a fair comparison for different filters, a normalisation on filter coefficients is required. In this paper, we assume that the designed filters have unity white noise gain, that is, the filter weights are normalised as $\alpha_i^n = \alpha_i / \sqrt{\sum_{i=0}^{N-1} \alpha_i^2}$. Here α_i^n is the normalised version of the weight α_i.

4 MTI filter design methodologies

For the generation of different trade-off points between the conflicting design objectives, three approaches are presented. The first approach is the LS approach. This approach aims to obtain a set of filter coefficients that approximate the desired response in the sense of minimum least-squared error. The second approach is based on the convex optimisation method (CVX). The third approach is based on the minimisation of the worst-case error and it is called as the MM error approach.

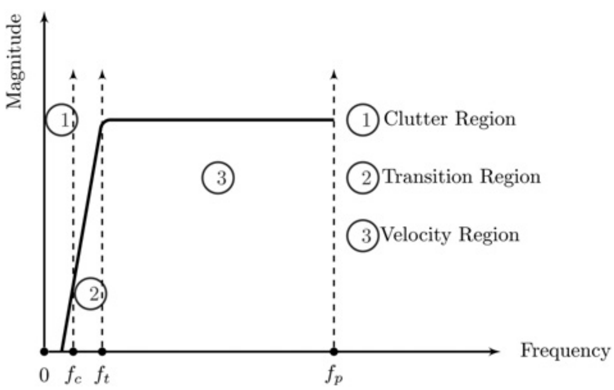

Fig. 3 *Ideal magnitude response for a non-uniformly sampled MTI filter*

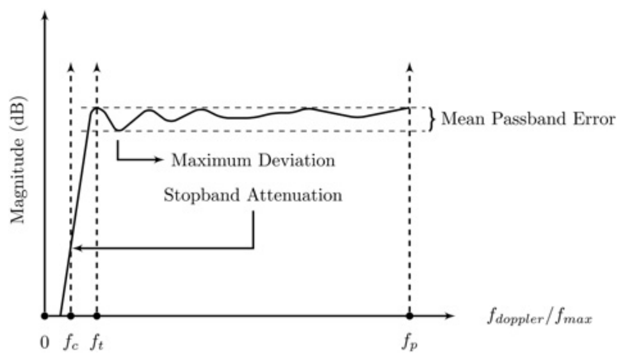

Fig. 4 *Performance measures of the staggered PRF MTI filter design*

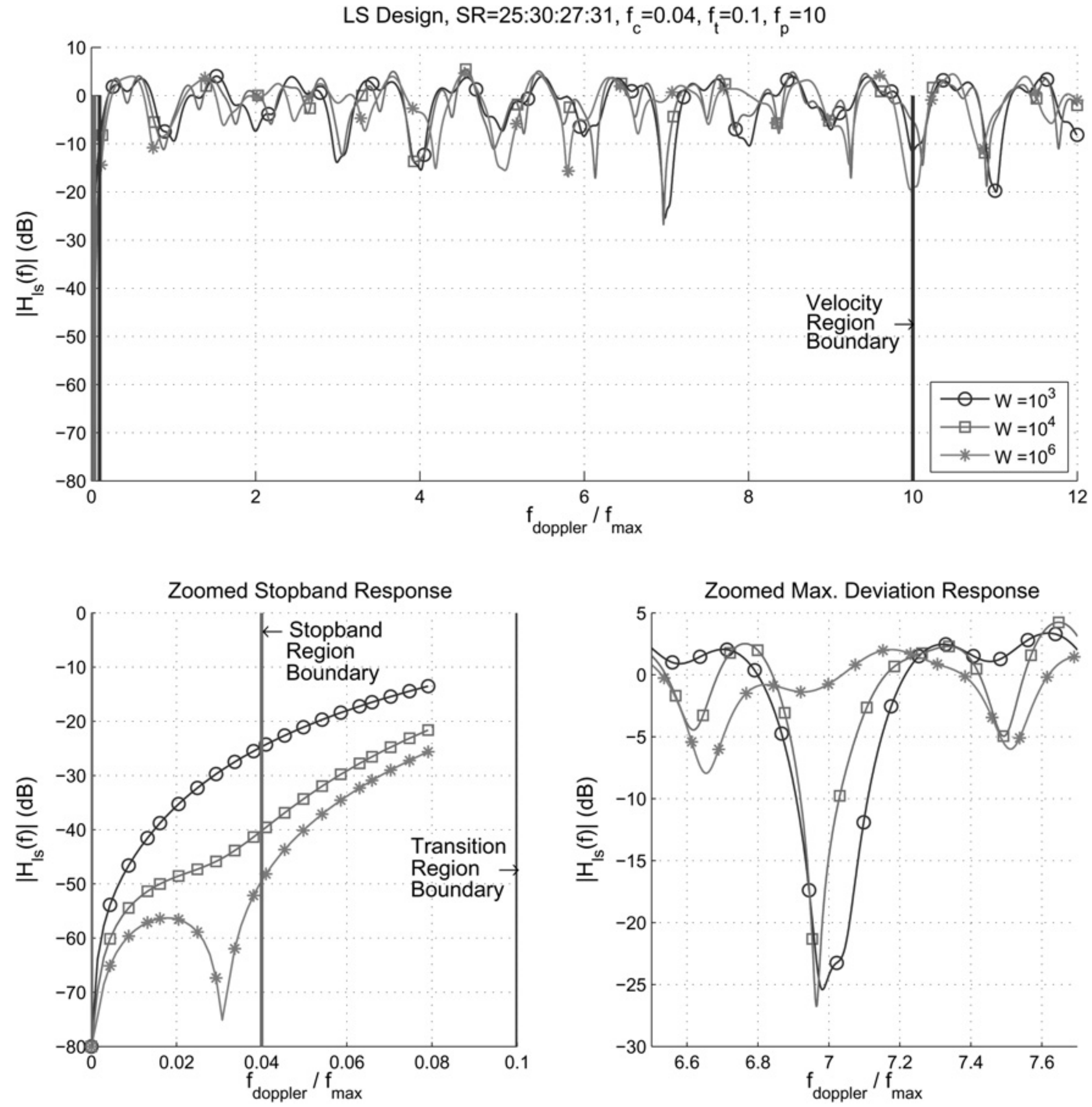

Fig. 5 *Frequency response of LSs based MTI filters for different weights*

4.1 LSs based design

The cost function for the LS sense design is given as follows:

$$J_{\text{cost}} = \int_0^{f_\text{d}} |H_\text{d}(f) - H_\text{ls}(f)|^2 \, \text{d}f = ||H_\text{d}(f) - H_\text{ls}(f,\ \alpha_i)||^2. \quad (7)$$

Here, $H_\text{d}(f)$ and $H_\text{ls}(f,\ \alpha_i)$ indicate the frequency responses of the desired and least-square sense designed filter, respectively. $H_\text{d}(f)$ is the ideal high-pass filter whose frequency domain definition given as

$$H_\text{d}(f) = \begin{cases} 0, & \text{if} \quad 0 \le f \le f_\text{c}, \\ 1, & \text{if} \quad f_t \le f \le f_p, \end{cases}. \quad (8)$$

Table 1 Performance measures of LSdesign-based MTI filters for different weights

W	SA, dB	MPE, dB	MD, dB
1000	−24.884	−0.659	25.409
10,000	−40.470	−0.699	26.771
1×10^6	−50.030	−0.691	19.569

The non-uniform MTI filter design problem can be written as

$$\begin{aligned} &\text{minimise} \ \ ||H_\text{d}(f) - H_\text{ls}(f,\ \alpha_i)||^2 \\ &\text{subject to} \ \sum_{i=0}^{N-1} \alpha_i = 0, \quad x \in \Re. \end{aligned} \quad (9)$$

Here, $||.||$ is the norm defined in (7); the constraint of $\sum_{i=0}^{N-1} \alpha_i = 0$ is provided to suppress the DC component. Using Lagrange multipliers λ, we can express the problem as follows:

$$J_{\text{cost}}(\alpha,\ \lambda) = \int_0^{f_\text{d}} \left| H_\text{d}(f) - \sum_{i=0}^{N-1} \alpha_i \text{e}^{-\text{j}2\pi f\, t_i} \right|^2 \text{d}f + \lambda \left(\sum_{i=0}^{N-1} \alpha_i \right). \quad (10)$$

By taking the partial derivatives of the cost function with respect to filter coefficients, we get

$$\frac{\partial J_{\text{cost}}}{\partial \alpha_i} = \int_0^{f_\text{d}} \left(H_\text{d}(f) - \sum_{n=0}^{N-1} \alpha_n \text{e}^{-\text{j}\pi f\, t_n} \right) \text{e}^{\text{j}2\pi f\, t_i} \, \text{d}f + \lambda. \quad (11)$$

By equating, the partial derivatives given in (11) to zero for

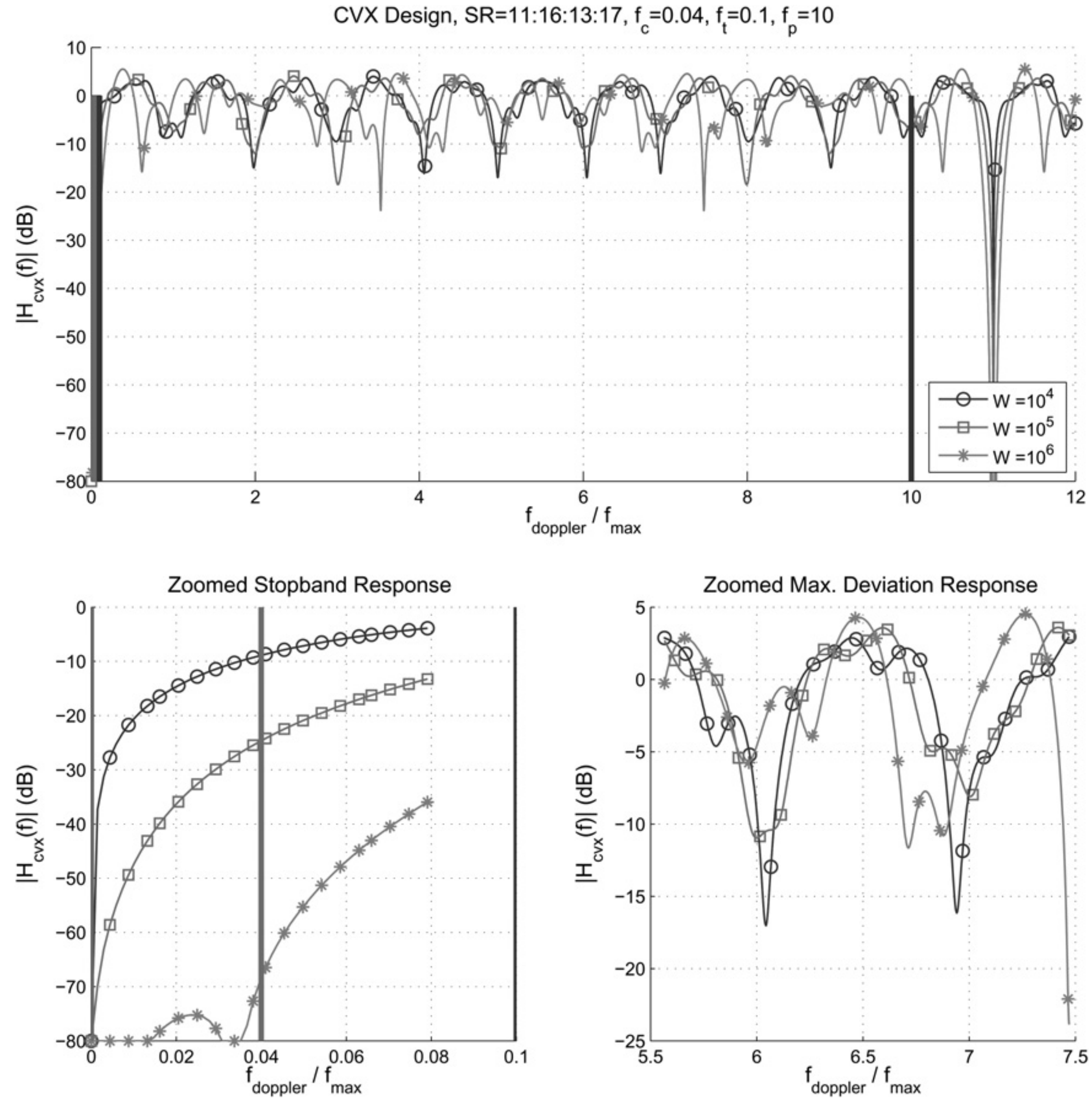

Fig. 6 *Frequency response of convex optimisation-based MTI filters for different weights*

$i = \{0,\ 1,\ \ldots,\ N\}$, we end up with a linear equation system

$$\boldsymbol{A}\boldsymbol{\alpha} = \boldsymbol{H}_{\mathrm{d}} + \imath\lambda\mathbf{1} \tag{12}$$

$\boldsymbol{H}_{\mathrm{d}}$ is an $N \times 1$ column vector with the kth entry $\boldsymbol{H}_{\mathrm{d}}(k) = \int_{f_{\mathrm{c}}}^{f_{\mathrm{d}}} \mathrm{e}^{\mathrm{j}2\pi f t_k}\,\mathrm{d}f$ and $\boldsymbol{A}$ is an $N \times N$ matrix with the ith row and jth column entry and $\boldsymbol{A}(i,\ j) = \int_0^{f_{\mathrm{d}}} \mathrm{e}^{-\mathrm{j}2\pi f(t_j - t_i)}\,\mathrm{d}f$ and $\mathbf{1}$ is the $N \times 1$ column vector composed of all ones $\mathbf{1} = [1\ \ 1\ldots1]^{\mathrm{T}}$. Finally, the vector $\boldsymbol{\alpha}$ in (12) is the vector of unknowns, that is, filter coefficients for the staggered system.

To establish a trade-off between the objectives of clutter attenuation and passband ripple; we introduce a weight W to control the contribution of the stopband error to the cost function

$$J_{\mathrm{cost}}^{W} = W \int_0^{f_{\mathrm{c}}} |H_{\mathrm{d}}(f) - H_{\mathrm{ls}}(f)|^2\,\mathrm{d}f + \int_{f_t}^{f_{\mathrm{d}}} |H_{\mathrm{d}}(f) - H_{\mathrm{ls}}(f)|^2\,\mathrm{d}f + \lambda\left(\sum_{i=0}^{N-1} \alpha_i\right). \tag{13}$$

The optimisation of the cost function results in the following equation system:

$$(W \times \boldsymbol{A}_{\mathrm{stop}} + \boldsymbol{A}_{\mathrm{pass}})\boldsymbol{\alpha} = \boldsymbol{H}_{\mathrm{d}} + \imath\lambda\mathbf{1}. \tag{14}$$

In the last equation, $\boldsymbol{A}_{\mathrm{stop}}(i,\ j) = \int_0^{f_{\mathrm{c}}} \mathrm{e}^{-\mathrm{j}2\pi f(t_j - t_i)}\,\mathrm{d}f$ and $\boldsymbol{A}_{\mathrm{pass}}(i,\ j) = \int_{f_t}^{f_{\mathrm{p}}} \mathrm{e}^{-\mathrm{j}2\pi f(t_j - t_i)}\,\mathrm{d}f$. It should be clear that by increasing W, the contribution of the stopband error to the cost function is increased. Therefore, for higher W values the optimised filter presents more clutter suppression by trading-off the passband performance.

Table 2 Performance measures of convex optimisation-based MTI filters for different weights

W	SA, dB	MPE, dB	MD, dB
10,000	−8.97	−0.617	17.016
100,000	−24.83	−0.667	18.457
1×10^6	−69.27	−0.626	27.632

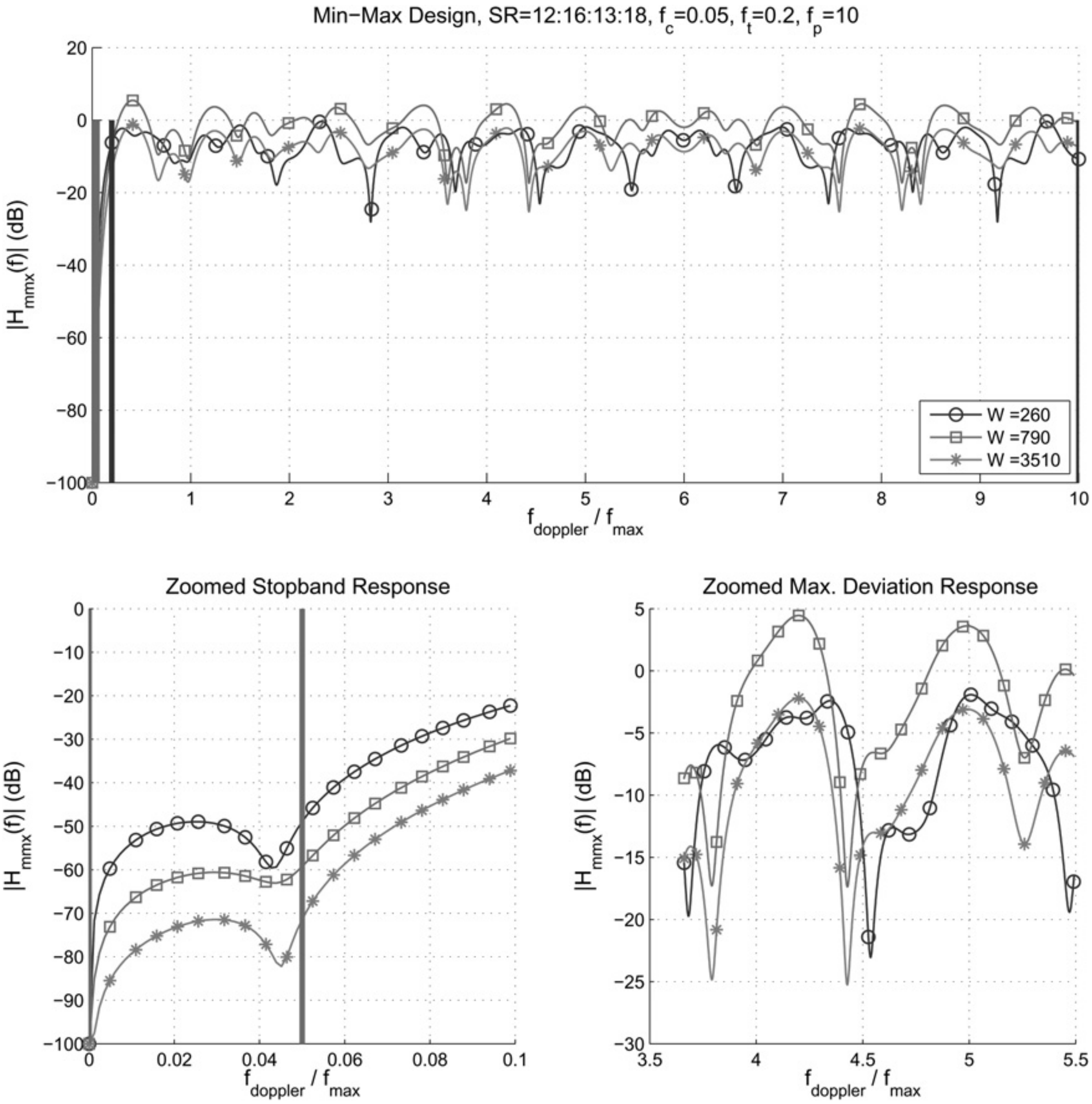

Fig. 7 *Frequency response of MM error design-based MTI filters for different weights*

By rewriting (14) as $\boldsymbol{\alpha} = (W \times \boldsymbol{A}_{\text{stop}} + \boldsymbol{A}_{\text{pass}})^{-1}(\boldsymbol{H}_{\text{d}} + \imath\lambda\mathbf{1})$ and using the constraint $\mathbf{1}^{\text{T}}\boldsymbol{\alpha} = 0$, the multiplier λ explicitly written as

$$\lambda = \frac{\mathbf{1}^{\text{T}}(W \times \boldsymbol{A}_{\text{stop}} + \boldsymbol{A}_{\text{pass}})^{-1}\boldsymbol{H}_{\text{d}}}{\mathbf{1}^{\text{T}}(W \times \boldsymbol{A}_{\text{stop}} + \boldsymbol{A}_{\text{pass}})^{-1}\mathbf{1}}. \tag{15}$$

To clarify the effect of weighting factor W, we present an example utilising the stagger ratios 25:30:27:31 given in [1]. Fig. 5 shows the results for the chosen stagger ratios. In this figure and following figures, the region boundaries are marked by bold vertical lines. From Fig. 5, it can be seen that an increase in the weight factor W results in a larger SA in the clutter region and larger MSE in the velocity region, as anticipated. However, the MD value does not change monotonously with W. This can be seen from the performance criterion in Table 1. (For $W = 10^3$, MD takes the value of 25.409 dB, whereas it is 19.569 dB when W equals to 10^6.) Since the value of MD is important to provide a good detection performance over the complete Doppler range, it is recommended to set the W value in accord with the achieved MD value.

Table 3 Performance measures of MM error design-based MTI filters for different weights

W	SA, dB	MPE, dB	MD, dB
260	−50.70	−6.28	28.07
790	−60.37	−0.57	17.53
3510	−73.86	−7.22	25.24

4.2 *Convex optimisation-based design*

We present a formulation for the staggered MTI filter design problem in the context of convex optimisation. Design objectives are similar to the LS sense design which is the minimisation of the passband error and maximisation of the SA. Similar to the LS design, a weight W is introduced to establish a trade-off between these objectives. The convex filter design problem can be written as follows: (see equation at bottom of the next page)

Here N is the order of the filter and the optimisation variables are the filter coefficients, $\alpha_i\ i = \{0,\ 1,\ \ldots,\ N-1\}$. The variables f_t and f_{d} are the lower and upper bounds of normalised passband frequency, respectively, and f_{c} is the upper bound of normalised stopband frequency as in Fig. 3. Similar to the LS design, an increase in the weight W increases the maximum tolerable passband ripple to $W\delta$ and this leads to the improvements in SA.

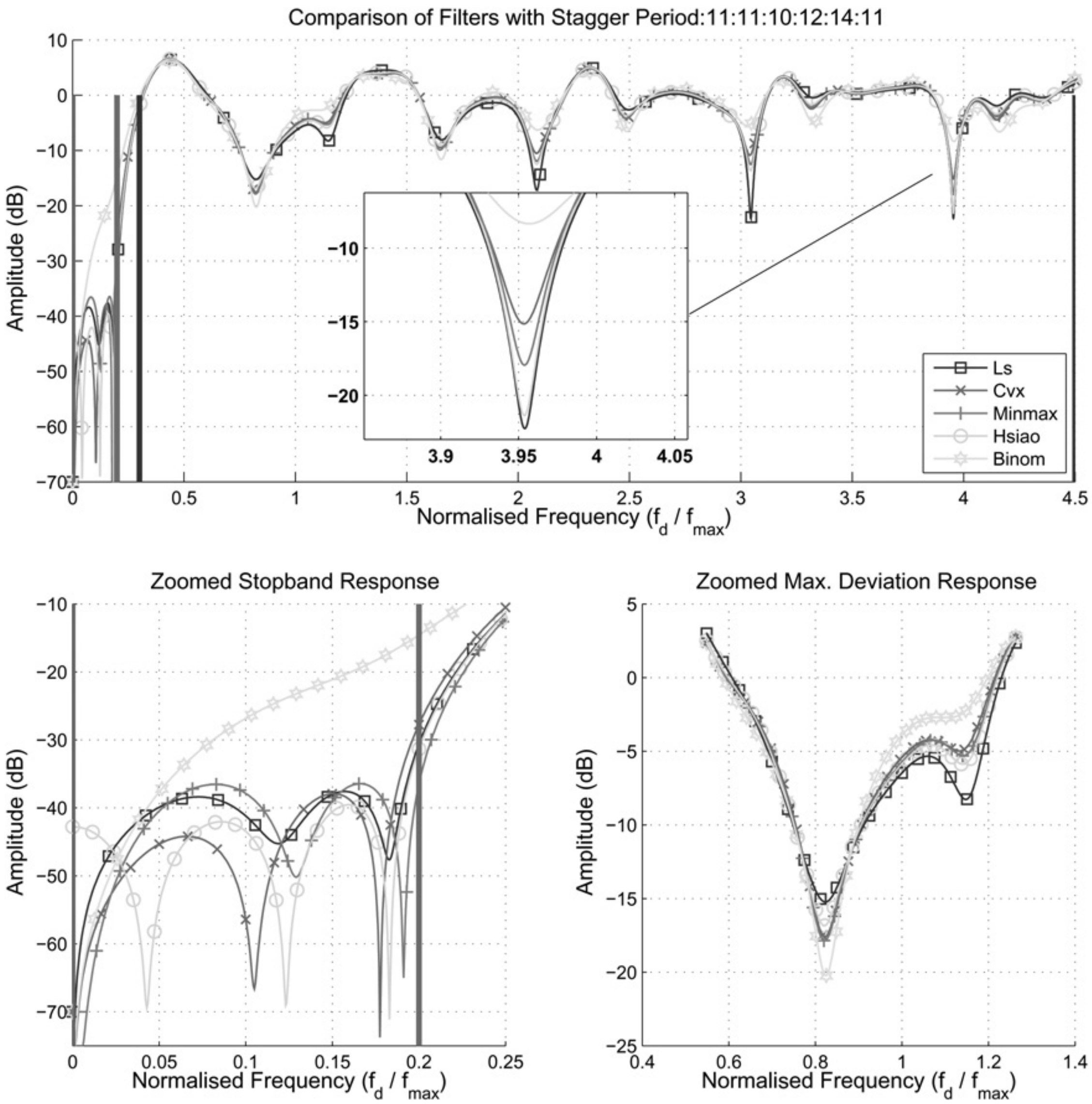

Fig. 8 *MTI filter frequency response for interpulse periods of [8]*

The convex optimisation problem can be expressed in the form given below which is compatible with the syntax of the off-the-shelf convex optimisation tool CVX [13] (see (16))

Different from the LS design, there is no closed-form solution for the convex optimisation problem. The optimisation has to be done numerically. The numerical implementation of the optimisation problem requires the discretisation of frequency band into a dense set of frequency points. Hence, the constraints given in (16) are not evaluated for a continuum of points; however, for a finitely many number of points. In the present paper, 8192 points are utilised in the discretisation of the frequency interval and the convergence to the global optima is rapid with the convex solver CVX available at [13].

$$\begin{aligned}&\text{minimise} && \delta\\ &\text{subject to} && |H(f,\ \alpha_i)| \le \delta,\ \ f \in [0,\ f_c],\ \ \alpha_i \in \boldsymbol{R},\ \ i \in \{0,\ 1,\ 2,\ \ldots,\ N-1\}\\ &&& |H(f,\ \alpha_i) - 1| \le W\delta,\ \ f \in [f_t,\ f_d],\ \ \alpha_i \in \boldsymbol{R},\ \ i \in \{0,\ 1,\ 2,\ \ldots,\ N-1\}\\ &&& \sum_{i=0}^{N-1} \alpha_i = 0,\ \ \alpha \in \boldsymbol{R}\end{aligned}$$

$$\begin{aligned}&\text{minimise} && \delta\\ &\text{subject to} && |\boldsymbol{A}_{\text{stop}}\boldsymbol{\alpha}| \le \delta,\ \ f \in [0,\ f_c],\ \ \alpha_i \in \boldsymbol{R},\ \ i \in \{0,\ 1,\ 2,\ \ldots,\ N-1\}\\ &&& |\boldsymbol{A}_{\text{pass}}\boldsymbol{\alpha} - \boldsymbol{1}| \le W\delta,\ \ f \in [f_t,\ f_d],\ \ \alpha_i \in \boldsymbol{R},\ \ i \in \{0,\ 1,\ 2,\ \ldots,\ N-1\}\\ &&& \sum_{i=0}^{N-1} \alpha_i = 0,\ \ \alpha \in \boldsymbol{R}\end{aligned} \tag{16}$$

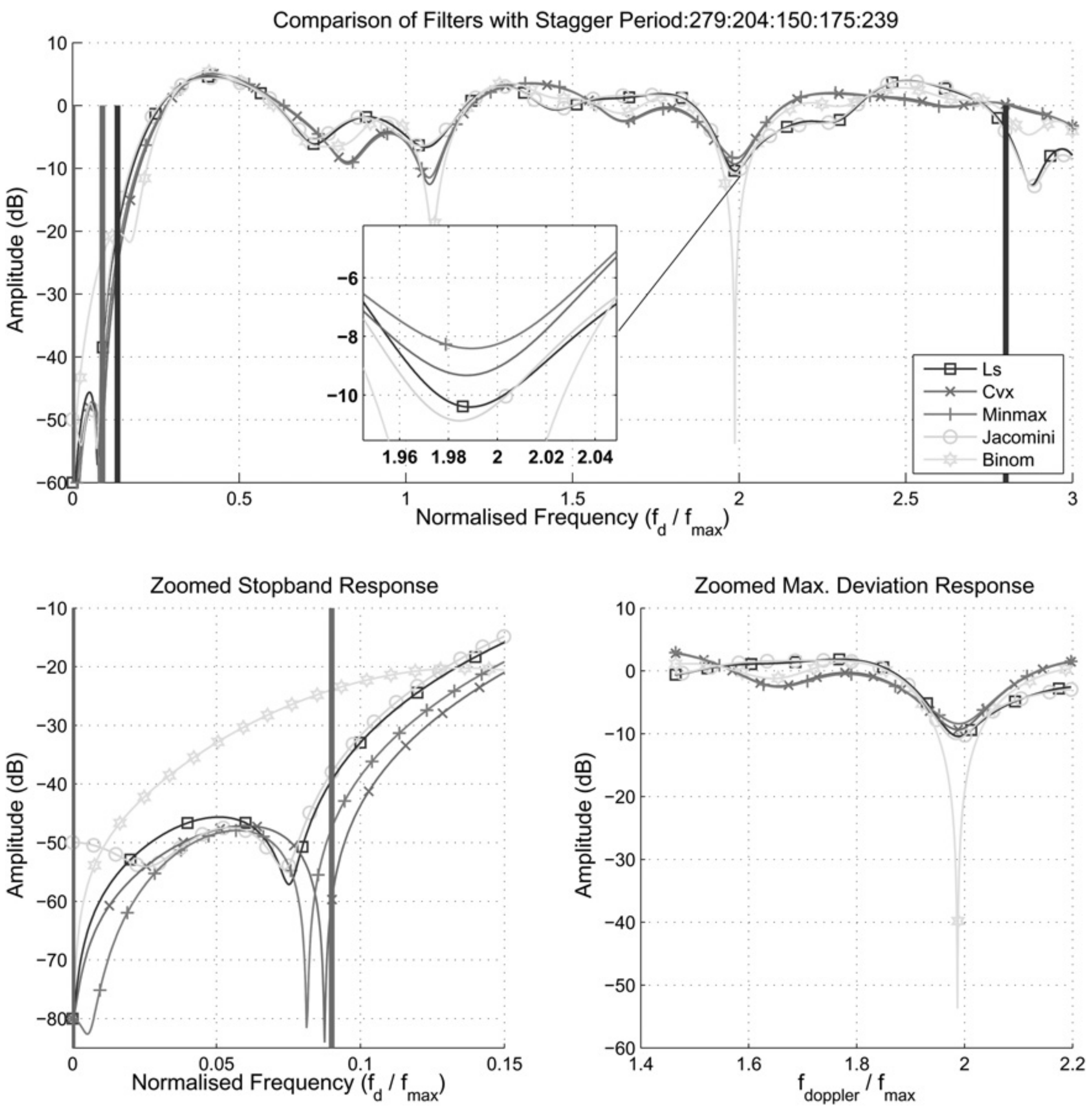

Fig. 9 *MTI filter frequency response for interpulse periods of [9]*

Fig. 6 indicates the frequency response of the designed non-uniform MTI filter for different W values and Table 2 gives the related performance criteria of the design. In this figure, the stagger ratios of 11:16:13:17 (taken from [1]) are utilised. As seen from Fig. 6, the effect of W on the SA is similar to the LSs based design. An increase in W improves the SA at the expense of passband deviations.

The weight factor of the convex optimisation-based design can be selected as in the LSs based design, that is, the weight W is increased so that the SA condition is satisfied and then, among the weight values satisfying the SA condition, the one with a smaller MD value can be selected.

4.3 MM error-based design

The MM error-based design aims to select the filter coefficients to minimise the MD from the desired response in the passband. This method exhibits an important difference when compared with earlier methods. The earlier designs yield a single global optima for every weight factor, while this MM error-based design exhibits several local maximas. Therefore, this method requires a good set of initial filter coefficients for a proper operation. Typically, we use the binomial filter coefficients, as explained below, as the initial filter coefficients. Some other initialisation choices are also discussed after the method description.

The problem of MM error-based filter can be written as follows: (see (17))

Here $H_{mm}(f,\ \alpha_i)$ is the frequency response of the MM filter and the variable δ shows the MD from the desired characteristics for $W = 1$. The goal in this design is to minimise the MD from the desired high-pass characteristic. The first and second constraints enforce the *magnitude deviation* to be smaller than δ (for $W = 1$) in the

$$\begin{aligned} &\text{minimise} \quad \delta \\ &\text{subject to} \quad |H_{mm}(f,\ \alpha_i)| \le \delta,\quad f \in [0,\ f_c],\quad \alpha_i \in \boldsymbol{R},\quad i \in \{0,\ 1,\ 2,\ \ldots,\ N-1\} \\ &\qquad\qquad \big|1 - |H_{mm}(f,\ \alpha_i)|\big| \le W\delta,\quad f \in [f_t,\ f_p],\quad \alpha_i \in \boldsymbol{R},\quad i \in \{0,\ 1,\ 2,\ \ldots,\ N-1\} \\ &\qquad\qquad \sum_{n=0}^{N-1} \alpha_n = 0,\quad \alpha \in \boldsymbol{R} \end{aligned} \tag{17}$$

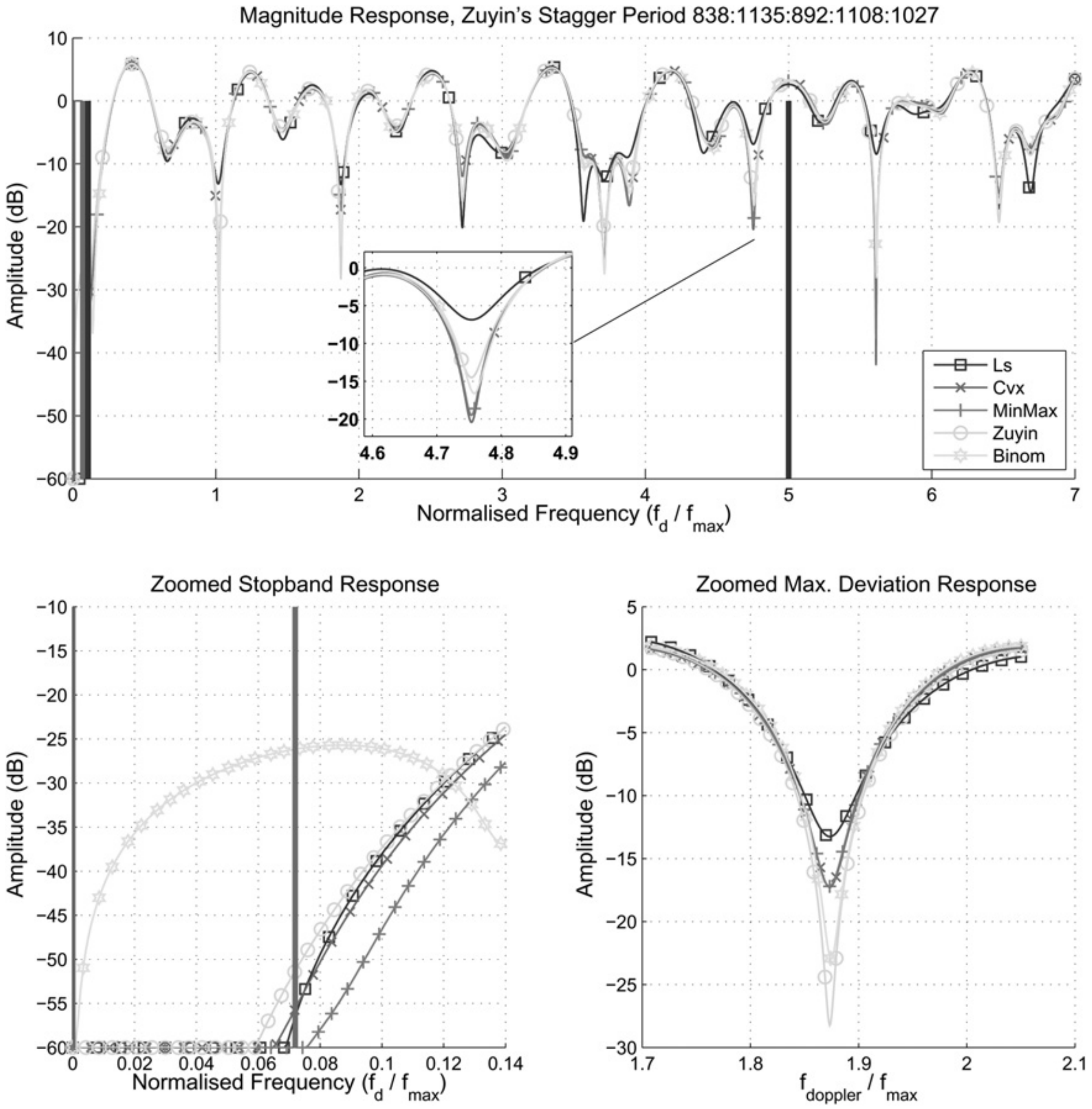

Fig. 10 *MTI filter frequency response for interpulse periods of [15]*

designated bands. The third constraint guarantees that the MM design has a null at DC frequency. Again a weight factor W is introduced to establish a trade-off between SA and passband ripple objectives. The presented figures are generated by using the binomial coefficients as the initial filter coefficients. (The binomial filter coefficients are the coefficients of the polynomial $(1-x)^N$.) The stagger ratios for this figure are 12:16:13:18 (taken from [14]).

Fig. 7 indicates the obtained frequency response for different weight factors and Table 3 gives the related performance measures of the design. We note that MM design requires more computation compared with the previous LS and convex design methods. The MM design of non-uniform MTI filter requires two phases. First, the weight factor is determined according to the required SA by using the binomial coefficients as the initial filter coefficients. After the weight factor selection, MM optimisation should be initiated with different initial conditions and the one with the minimum deviation in the passband should be selected as the final filter. With this approach, it is possible to obtain desired SA with a better passband characteristics.

Previously, it has been suggested to use the binomial filter coefficients as the initial weights for the optimisation procedure. In addition to this choice, it is possible to use randomly selected weights or randomly selected weights with the constraint that the sum of the weights (DC gain of the filter) is equal to zero can also be utilised. Depending on the application scenario (i.e. stagger ratio and filter specifications) one initialisation method may yield a better solution over another one.

5 Numerical comparisons

In this section, we present some numerical comparisons of the suggested designs with the available optimised MTI filters in the literature. We take the optimised filters of Hsiao, Jacomini and Zuyin's as reference designs from the literature [8, 9, 15]. It should be noted that stagger periods given in the reference works are different from each other. We individually compare the proposed filters with the optimised filters of Hsiao, Jacomini and Zuyin in three sets of experiments whose results are shown in Figs. 8–10 and then present a comparison on the IF of the filters in Fig. 11.

5.1 Frequency response comparisons

The results of first experiment are given in Fig. 8 and Table 4. It can be noted that the MM design presents 5.22 dB better attenuation (SA) than Hsiao's design and has almost the same passband

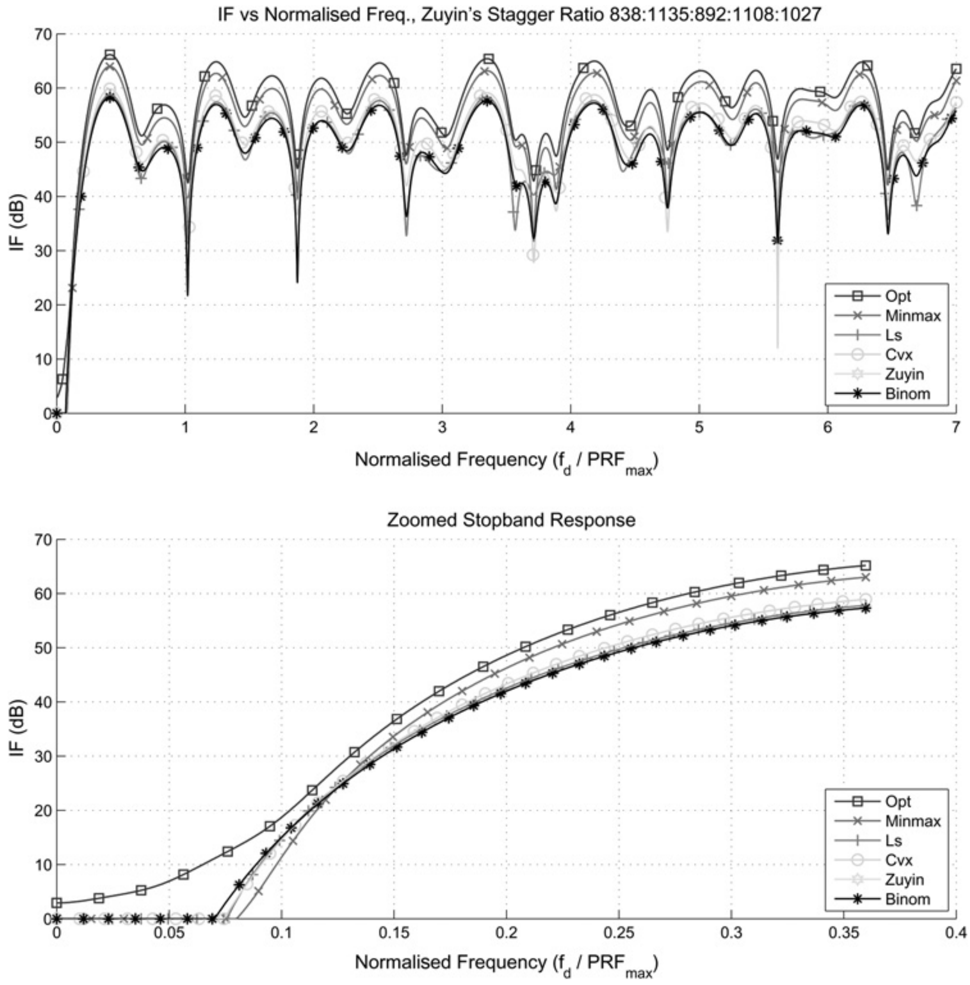

Fig. 11 *MTI IF comparison*

Table 4 Performance comparison (interpulse periods are from [8])

	SA, dB	MPE, dB	MD, dB
LS	−30.66	**−0.6012**	22.32
convex	−27.75	−0.5432	17.59
MM	**−36.55**	−0.5696	17.95
Hsiao and Kretschmer [8]	−31.33	−0.5704	21.37
binomial	−14.57	−0.5133	20.23

performance. Fig. 9 shows the results of second experiment. Here, the suggested designs are compared with the one given in [9]. In this comparison, the staggering periods [279, 204, 150, 175, 230] appearing in the title of Fig. 9 are the utilised values by Jacomini in [9] and represent the interpulse periods in milliseconds. (The corresponding sampling times t_k for this scenario becomes [0.0, 0.279, 0.483, 0.633, 0.808, 1.047] s.) When the responses in Fig. 9 and Table 5 are compared, we can say that LS design yields a similar performance to the design given in [9]. This is expected due to similarity in the cost functions and objectives of both methods. Compared with the LS design, convex optimisation based and MM error-based designs achieve significantly better responses for SA and MPE criterions.

The last frequency response comparison is given in Fig. 10 and Table 6. Here Zuyin's design given in [15] is compared with the suggested designs. It can be noted that MM design presents a significant gain in SA and yields a better performance in passband in comparison with the other designs. It can be seen from Table 6 that MD and SA values are improved by 2–11 dB compared with the Zuyin's. The numerical values for filters designed according to the described methodologies can be found in [12, Appendix A].

5.2 IF comparisons

As discussed in Section 2, the IF is the ratio of SCR values at the input and output of the MTI filter. It should be underlined that MTI filters are designed to suppress the clutter signal, but their application also leads to a suppression of desired signal to some degree. The IF is a measure indicating the effectiveness of the clutter removal at the expense of desired signal attenuation.

Table 5 Performance comparison (interpulse periods are from [9])

	SA, dB	MPE, dB	MD, dB
LS	−39.61	−0.0262	**10.41**
convex	**−61.13**	**−0.2525**	13.84
MM	−47.91	−0.2512	12.64
Jacomini [9]	−38.25	−0.0139	10.88
binomial	−24	−0.2436	53.72

Table 6 Performance comparison (interpulse periods are from [15])

	SA, dB	MPE, dB	MD, dB
LS	−56.71	−1.108	38.05
convex	−55.75	−1.152	39.04
MM	**−62.05**	**−1.175**	46.62
Zuyin [15]	−51.43	−1.154	37.36
binomial	−26.17	−1.19	41.37

Table 7 MTI IF comparison (interpulse periods are from [15])

	Optimum	MM	LS	CVX	Zuyin	Binomial
IF, dB	56.887	54.298	49.525	50.375	48.701	48.701

Fig. 11 shows the IF curves for the suggested filter designs. Here, the clutter is assumed to have a Gaussian distributed power spectral density, as in (4). Since the clutter power spectral density is not bandlimited, the clutter signal has a negative impact over the complete Doppler spectrum. Our goal in the presented IF comparison is to show the effectiveness of MTI filtering, that is, the increase in SCR via MTI operation, for different target Doppler frequencies.

It should be noted that the optimum filter maximising output SCR for a specific target Doppler frequency (the linear combiner maximising IF at a particular Doppler frequency) can be analytically expressed as $\boldsymbol{w}_{\text{opt}} = \boldsymbol{R}_{cn}^{-1}\boldsymbol{s}(\omega)$ [11, Sec. 5.2.5]. Here, $\boldsymbol{R}_{cn}$ is the normalised auto-correlation matrix of the clutter and $\boldsymbol{s}(\omega)$ is the desired signal vector, containing the slow-time samples (non-uniformly sampled) of target echo, as discussed in Section 2. Fig. 11 includes the IF curves of the optimal system. The IF curve for the optimal combiner is given as a benchmark or as an upper bound for performance improvement. In practice, the performance of the optimal system is not achievable, since the clutter power is not exactly Gaussian distributed and even if it is Gaussian distributed, its parameters cannot be exactly estimated. Yet, the upper bound on MTI IF can be useful to assess the 'suitability' of an MTI filter to a specific application scenario.

The filters designed by proposed methods are adjusted to have a cut-off frequency which is two times the Doppler spread of clutter, that is, $f_c = 2\sigma_g$, where σ_g is the parameter in (4) associated with the clutter Doppler spread. It can be noted from Fig. 11 that the MM filter presents an IF value which is quite close to the performance upper bound at almost all Doppler frequencies. The average MTI IF values for different designs are provided in Table 7. The average values of the IF curves can be interpreted as the MTI gain for a target with a random Doppler frequency which is known to be uniformly distributed in the Doppler range of interest. The results in Table 7 show that there can be a significant gain on the application of a suitable MTI filter with respect to this metric.

6 Conclusions

The present paper examines the problem of MTI filter design for the systems utilising staggered PRIs. Three well-known filter design methods, the LSs design, convex optimisation-based design and MM error-based design, have been considered. The results indicate that with a proper selection of a weight parameter, a good compromise between clutter attenuation and flat passband response can be attained for different scenarios.

We note that the MM design (or its relaxed version convex optimisation-based design) can yield a similar or a better performance than highly optimised filters available in the literature with a proper selection of weight factor. This is indeed an important result since the utilisation of the generic optimisation routines can significantly shorten and simplify the filter design cycles. Interested readers can also examine [12] for additional simulation results and further details on the design procedures.

It should be underlined that the filter designs suggested in the present paper are specific to a given set of stagger periods. Yet, the presented design methods can be used to jointly optimise the stagger periods, MTI filter order and its coefficients. That is, among a set of possible stagger sequences covering the same unambiguous Doppler range, the one whose optimised MTI response is closest to the desired response can be selected in an automated way. Such an operation may result in a dynamic procedure for the MTI filter selection according to existing clutter conditions. The joint optimisation of stagger periods, filter order and its coefficients can be pointed as a venue for further research complementing the present paper.

As a final remark, we note that a ready-to-use MATLAB code for the suggested designs is provided in [10].

7 References

1 Skolnik, M.I.: 'Introduction to radar systems' (McGraw-Hill, New York, 2001, 3rd edn.)

2 Schleher, D.C.: 'MTI and pulsed Doppler radar with MATLAB' (Artech House, Boston, MA, 2010)

3 Prinsen, P.J.A.: 'A class of high-pass digital MTI filters with nonuniform PRF', *Proc. IEEE*, 1973, **61**, (8), pp. 1147–1148

4 Prinsen, P.J.A.: 'Elimination of blind velocities of MTI radar by modulating the interpulse period', *IEEE Trans. Aerosp. Electron. Syst.*, 1973, **AES-9**, (5), pp. 714–724

5 Banjanin, Z.B., Zrnic, D.S.: 'Clutter rejection for Doppler weather radars which use staggered pulses', *IEEE Trans. Geosci. Remote Sens.*, 1991, **29**, (4), pp. 610–620

6 Bidégaray-Fesquet, B., Fesquet, L.: 'A fully nonuniform approach to FIR filtering'. SAMPTA'09, Int. Conf. on Sampling Theory and Applications, Marseille, France, 2009

7 Jin, Z., Li, X.-D., King, J.: 'Non-uniform time sampling FIR filter design based on least-squares criterion', *Electron. Lett.*, 2010, **46**, (23), pp. 1544–1545

8 Hsiao, J.K., Kretschmer, F.F. Jr.: 'Design of a staggered-PRF MTI Filter'. Defense Technical Information Centre, 1973

9 Jacomini, O.J.: 'Weighting factor and transmission time optimization in video MTI radar', *IEEE Trans. Aerosp. Electron. Syst.*, 1972, **AES-8**, (4), pp. 517–527

10 Ispir, M., Candan, C.: 'On the design of staggered moving target indicator (MTI) filters, MATLAB code'. Available at http://www.eee.metu.edu.tr/ccandan/pub.htm, accessed March 2015

11 Richards, M.A.: 'Fundamentals of radar signal processing' (McGraw-Hill, New York, NY, 2005), pp. 239–242

12 Ispir, M.: 'Design of moving target indication filters with non-uniform pulse repetition intervals'. Master's thesis, Middle East Technical University, 2013

13 Grant, M., Boyd, S.: 'CVX: Matlab software for disciplined convex programming, version 2.1'. Available at http://www.cvxr.com/cvx/, accessed 2014

14 Thomas, H.W., Abram, T.M.: 'Stagger period selection for moving-target radars', *Proc. Inst. Electr. Eng.*, 1976, **123**, (3), pp. 195–199

15 Zuyin, W.: 'Optimal design of clutter rejection filters for MTI system'. Int. Conf. on CIE, 2001, pp. 475–478